

Chapter 2

A Soft-Switching Control Method of Isolated LC Series Resonant Transformer Full Bridge DC–DC Converter

Meng Jiang and Wei Li

Abstract For the different characteristics of nonresonant and resonant isolated bidirectional full bridge DC–DC converter, a unified expression of power transmissions is derived from two DC–DC converters. The power transfer characteristics could be unified described through the power expression. The problem of isolated bidirectional DC–DC converter is that the switching loss increases and the converter efficiency declines with the forced turn-on or turn-off of switch devices in high-frequency situation. In this paper, to solve this problem, an isolated LC series resonant transformer full bridge DC–DC converter is taken as research object, a phase-shift control strategy which could realize zero voltage turn-on and decrease the turn-off current of the power devices to decrease switching loss and increase the efficiency is proposed. The validity of proposed control strategy is verified through simulation and experiment results.

Keywords Bidirectional full bridge DC–DC converter · Series resonant · Soft-switching technology · First harmonic analysis · Voltage gain

2.1 Introduction

The isolated bidirectional full bridge DC/DC converter, known as Dual Active Bridge (DAB), has the advantages that medium (or high) frequency transformer could realize electrical isolation, which improves system reliability, and soft

M. Jiang (✉)

Management Department, Tianjin University, 92 Weijin Road, Nankai District, Tianjin, People's Republic of China
e-mail: jiangmeng168@163.com

M. Jiang · W. Li

Rescuing Center for Mineral Disaster of Henan, No. 116, East Second Street, Zhengzhou, People's Republic of China

switch control of both primary side and secondary side of transformer that could reduce system loss. Bidirectional energy flow of converter could be achieved. High frequency transformer is used to replace the power frequency transformer, which could reduce the size and mass and improve power density of the system. Such converters are widely used in applications like power electronic transformer [1], locomotive traction [2], renewable energy power generation [3], high voltage motor drive [4, 5].

DC–DC converter, which is an important unit of power electronic transformer is utilized to achieve electrical isolation and voltage level conversion. According to the different topologies, it could be divided into nonresonant and resonant DC–DC converters. According the different control strategies, it could be divided into phase-shift control and combination of phase-shift and PWM modulation [6–12].

The main work in this paper is listed as:

- (1) The unified power transfer expression, which could describe the relationship of resonant and nonresonant DC–DC converter, is derived in this paper. The derived expression helps in modeling and Analysis of DC–DC converter.
- (2) Through the comparison and analysis of nonresonant and resonant DC–DC converter, a control strategy based on phase-shift control for resonant DC–DC converter is proposed in this paper.

2.2 The Principle of DC/DC Converter

Figure 2.1 shows the topology of an isolated LC series resonant transformer full bridge DC/DC converter. It consists of two active full bridges, a series resonance unit and an isolation transformer. L_r is the equivalent of primary and secondary leakage inductance of high frequency transformer. U_{ab} and U_{cd} are 50 % duty cycle square waves. ϕ is the phase-shift angle of U_{ab} and U_{cd} .

Considering the affection of line impedance of LC series resonance circuit and magnetic inductance of transformer, the approximate equivalent circuit and its phasor diagram of DC–DC converter is shown in Figs. 2.2 and 2.3.

where θ , β , ϕ are respectively phase differences among current i_r , voltage U_{ab} , u'_{cd} . U_{ab_f} and u'_{cd_f} are respectively the fundamental component of voltage U_{ab} and u'_{cd} . Z_{eq} is the equivalent impedance of R_o in the equivalent circuit.

Set ω_r , ω_s are resonant angular frequency and switching frequency, f_r , f_s are resonant frequency and switching frequency, n is turns ratio of transformer.

The fundamental of u_{ab} and u_{cd} , which are defined as u_{ab_f} and u_{cd_f} , could be expressed as follows:

$$u_{ab_f}(t) = \frac{4}{\pi} U_i \cos \omega_s t \quad (2.1)$$

$$u_{cd_f}(t) = \frac{4}{\pi} U_o \cos(\omega_s t - \phi) \quad (2.2)$$

Fig. 2.1 Isolated bidirectional full bridge DC/DC converter

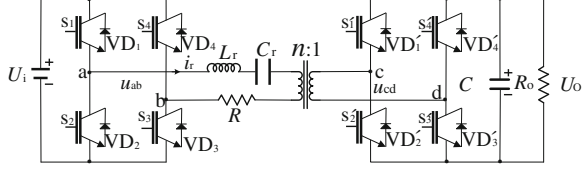


Fig. 2.2 Approximate equivalent circuit of DC-DC converter

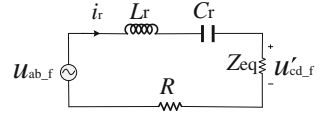
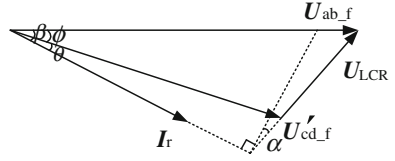


Fig. 2.3 Phasor diagram of the equivalent circuit



In the approximate equivalent circuit, u'_{cd_f} could be expressed as

$$u'_{cd_f}(t) = \frac{4}{\pi} U'_o \cos(\omega_s t - \phi) \quad (2.3)$$

The Impedance of R , L_r and C_r in the LRC resonant circuit could be derived as

$$Z = R + j(\omega_s L_r - \frac{1}{\omega_s C_r}) = |Z| \angle (90^\circ - \alpha) \quad (2.4)$$

$$|Z| = \sqrt{R^2 + (\omega_s L_r - \frac{1}{\omega_s C_r})^2} \quad (2.5)$$

So

$$i_r = \frac{\dot{U}_{ab_f} - \dot{U}'_{cd_f}}{Z} = \frac{2\sqrt{2}}{\pi|Z|} (U_i \angle (\omega_s t - 90^\circ + \alpha) - U'_o \angle (\omega_s t - \phi - 90^\circ + \alpha)) \quad (2.6)$$

The output instantaneous power p_o , which is transferred through the secondary of transformer, could be derived as

$$p_o = u'_{cd_f}(t) i_r(t) = \frac{16nU_o}{\pi^2 \sqrt{R^2 + (\omega_s L_r - \frac{1}{\omega_s C_r})^2}}.$$

$$\left\{ \frac{1}{2} U_i [-\sin(2\omega t + \alpha - \phi) + \sin(\phi + \alpha)] - \frac{1}{2} U_o' [-\sin(2\omega t + \alpha - 2\phi) + \sin \alpha] \right\} \quad (2.7)$$

Considering $U_o' = nU_o$, in the $0 \sim T$ period, the average power P_o of DC–DC converter could re-expressed as

$$P_o = \frac{8nU_o[U_i \sin(\phi + \alpha) - nU_o \sin \alpha]}{\pi^2 \sqrt{R^2 + (\omega_s L_r - \frac{1}{\omega_s C_r})^2}} \quad (2.8)$$

Set $F = \frac{\omega_s}{\omega_r} = \frac{f_s}{f_r}$, $Q = \frac{\omega_r L_r}{R_o}$, so $\frac{\omega_s L_r}{R_o} = QF$ $\frac{1}{\omega_s C_r R_o} = \frac{Q}{F}$

The average output power P_o is derived as

$$P_o = \frac{8n \cdot U_o \cdot [U_i \cdot \sin(\phi + \alpha) - nU_o \sin \alpha]}{\pi^2 \sqrt{R^2 + (w_r L_r)^2 \cdot (F - 1/F)^2}} \quad (2.9)$$

Formula (2.9) indicates that the average transfer power of DC/DC converter is determined by phase-shift ϕ and output voltage U_o .

2.3 Traditional Control Method of DC–DC Converter and Existing Problem

Traditional topology of DC–DC converter is shown in Fig. 2.4, where R is the circuit impedance, L is the leakage inductance of high frequency isolated transformer.

From formula (2.9), in nonresonant situation, the converter output power P_o is re-expressed as

$$P_o = \frac{8n \cdot U_o \cdot U_i}{\pi^2 \cdot w_s \cdot L} \sin \phi \quad (2.10)$$

Under PWM modulation, the typical waveforms of voltage U_{ab} and current i_r is shown in Fig. 2.5.

From Fig. 2.5, the turn-off current is very high in hard-switching mode. The forced shut-off mode of switching devices is called hard-switching. The circuit structure is simple, however, the switching loss is greater.

2.4 Improved Control Method of DC–DC Converter

To decrease the switching loss and improve converter efficiency, in this paper, an isolated LC series resonant transformer full bridge DC/DC converter, which is

Fig. 2.4 Nonresonant bidirectional full bridge DC–DC converter

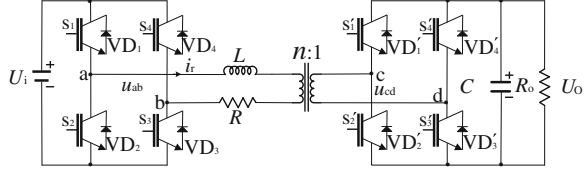
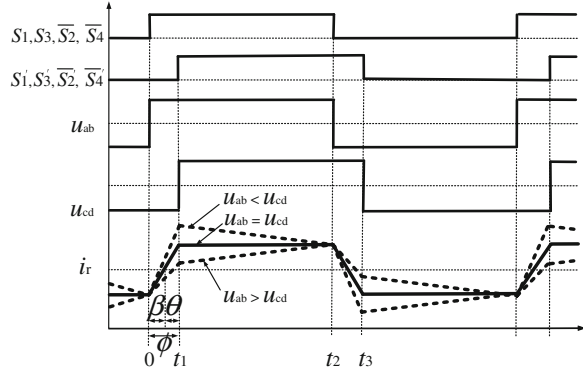


Fig. 2.5 Waveforms of U_{ab} , U_{cd} and i_r in hard-switching mode



shown in Fig. 2.1, is taken into research. Two power transmission modes are given based on analysis of formula (2.9).

2.4.1 Synchronous Control Mode

If $F = 1$, $\phi = 0$, formula (2.9) is expressed as

$$P_o = \frac{8n \cdot U_o}{\pi^2 \cdot R} (U_i - n \cdot U_o) \quad (2.11)$$

From the output load power:

$$P_{\text{load}} = \frac{U_o^2}{R_o} \quad (2.12)$$

From formula (2.11) and (2.12), the transmission power could be re-expressed as

$$P_o = \frac{8n \cdot U_i \cdot R_o}{8n^2 R_o + \pi^2 R} \quad (2.13)$$

Formula (2.13) indicates that power transmission is determined by differential of input and output voltage in synchronous mode. The output voltage U_o is determined by load R_o . Assuming the turn ratio of transformer is 1, the typical waveforms of voltage U_{ab} and current i_r is shown in Fig. 2.6.

Fig. 2.6 Waveforms of U_{ab} , U_{cd} and i_r in synchronous control mode

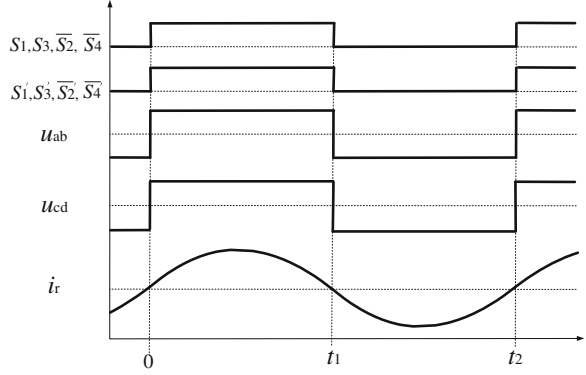


Figure 2.6 indicates that it is a synchronization action for switching devices of both primary and secondary sides under such power transmission mode. The output voltage U_o is determined by load R_o . This method is suitable for the situation that the variation range of U_o is not great.

2.4.2 Phase-Shift Control Method

If $F \neq 1$, $\phi \neq 0$, neglecting circuit impedance, $\alpha = 0$, the average transmission power P_o could be described as

$$P_o = \frac{8n \cdot U_o \cdot U_i}{\pi^2 \cdot (w_s L_r - \frac{1}{w_s C_r})} \quad (2.14)$$

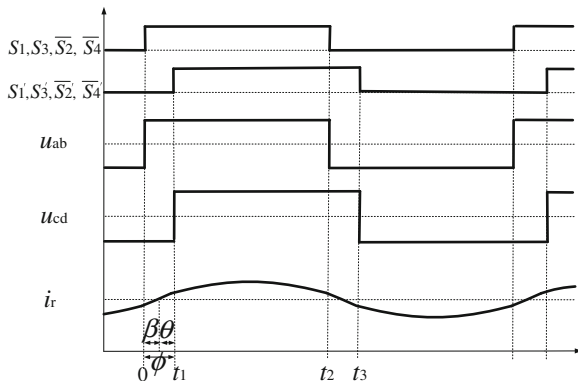
Via adjusting phase-shift ϕ , the output power P_o and output voltage U_o could be closed-loop controlled. Assuming the turn ratio of transformer is 1, the typical waveforms of voltage U_{ab} and current i_r is shown in Fig. 2.7.

The voltage gain of the equivalent circuit, namely the ratio of output voltage and input voltage could be defined as

$$M = \frac{|U'_{cd_f}|}{|U_{ab_f}|} \quad (2.15)$$

Figure 2.7 shows that when $\omega_s t = 0$, $i_r(0) < 0$, namely $\sin(-\beta) < 0$, the primary side achieved ZVS and when $\omega_s t = \phi$, $i_r(t_1) > 0$, namely $\sin(-\theta) < 0$, the secondary side achieved ZVS. So constraint equations of soft switch could be derived as follows:

Fig. 2.7 Waveforms of U_{ab} , U_{cd} and i_r in phase-shift control mode



$$\begin{cases} M \cos \phi - 1 < 0 \\ M - \cos \phi > 0 \end{cases} \quad (2.16)$$

If only $M = 1$, the equations could be satisfied. In this mode, the realization of soft-switching is independent of the load. It means that ZVS of primary side and secondary side could be achieved over a wide load range.

2.5 Simulation and Experiment

2.5.1 Simulation

From the above theoretical analysis, PSIM is utilized to verify the proposed strategy. The simulation parameters are list as the following.

In nonresonant situation, L is 30 μH , switching frequency f_s is 6 kHz, load R_o is 7 Ω . The input voltage U_i is, respectively, set to 50 V and 100 V, (corresponding output power 0.36 kW and 1.43 kW), the waveforms of driving signal, U_{ab} , U_{cd} and i_r are shown in Figs. 2.8 and 2.9.

In resonant situation, the resonant inductor L_r is 30 μH , resonant capacitor C_r is 20 μF , resonant frequency f_r is 5.3 kHz, switching frequency f_s is 6 kHz, load R_o is 7 Ω . When input voltage U_i is, respectively, set to 50 and 100 V, (corresponding output power is 0.36 and 1.43 kW), the waveforms of driving signal, U_{ab} , U_{cd} and i_r are shown in Figs. 2.10 and 2.11.

Fig. 2.8 Waveforms of U_{ab} , U_{cd} and i_r when $U_i = 50$ V

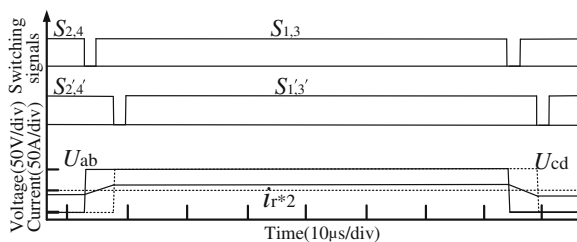


Fig. 2.9 Waveforms of U_{ab} , U_{cd} and i_r when $U_i = 100$ V

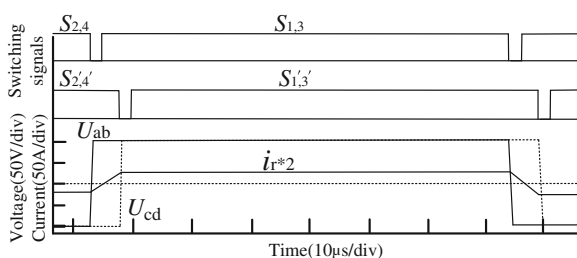


Fig. 2.10 Waveforms of U_{ab} , U_{cd} and i_r when $U_i = 50$ V

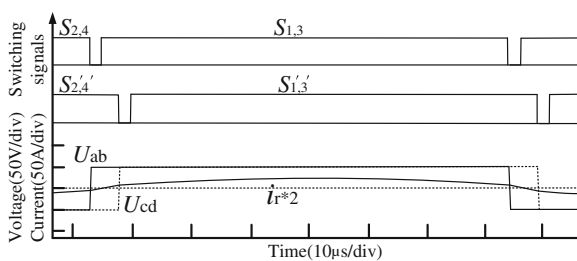


Fig. 2.11 Waveforms of U_{ab} , U_{cd} and i_r when $U_i = 100$ V

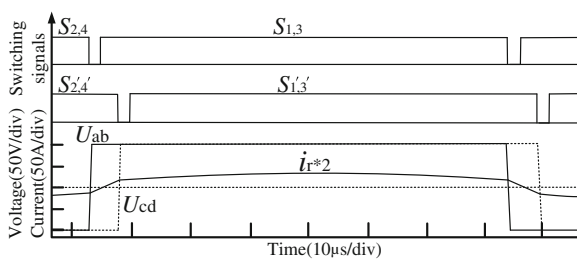


Fig. 2.12 Waveforms of U_{ab} , U_{cd} and i_r when $U_i = 50$ V

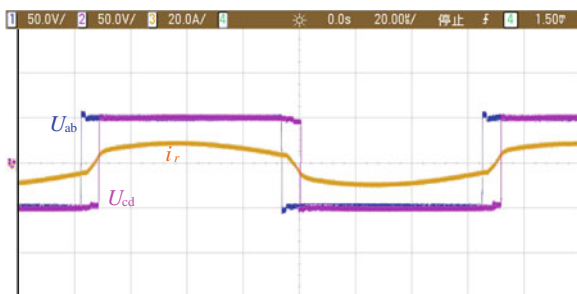


Fig. 2.13 U_{ab} , U_{cd} and i_r when $U_i = 50$ V

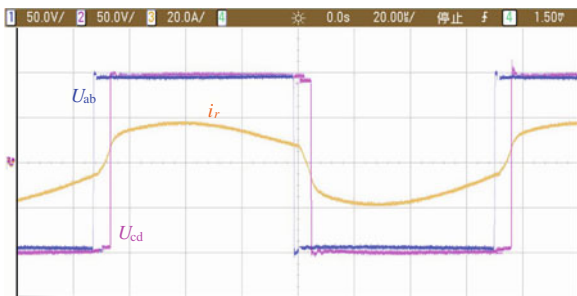
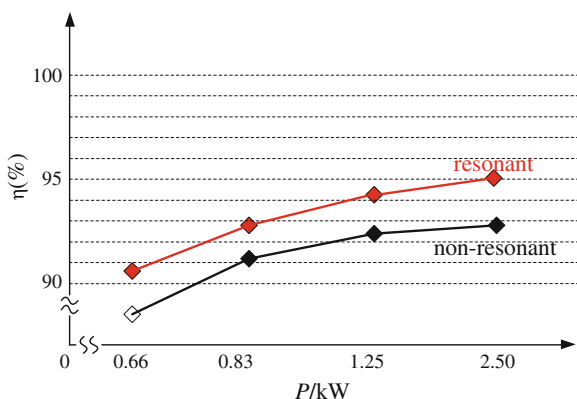


Fig. 2.14 Efficiency curves of DC–DC converter



2.5.2 Experiment

The parameters of actual circuit are as follows: transformer turns ratio $r = 1$, $L_s = 30 \mu\text{H}$, $P_s = 10 \text{ kW}$, $L_r = 15 \mu\text{H}$, $C_r = 20 \mu\text{F}$, $R_o = 7 \Omega$, $f_s = 6 \text{ kHz}$, $f_r = 5.3 \text{ kHz}$, $t_{\text{dead}} = 2 \mu\text{s}$.

Where r is transformer ratio, P_s is rated power, t_{dead} is switching tube dead-time.

Figures 2.12 and 2.13 shows the waveforms of U_{ab} , U_{cd} and i_r when input voltage is respectively 50 and 100 V.

In order to verify the efficiency of soft-switching of the system, experiment curves are depicted to calculate system efficiency in non-resonant mode and resonant mode. The output power are, respectively 0.36, 1.43, 3.21 and 5.71 kW. Comparison results are shown in Fig. 2.14.

Experiments results indicate that the efficiency is higher under resonant mode.

2.6 Conclusion

Based on the comparison of power transfer mode and control features for non-resonant and LC resonant DC–DC converter, the conclusion is:

- (1) The proposed power transfer unified expression could describe the power transmission characteristics of nonresonant and resonant DC–DC converter in one formula. This expression is helpful for analysis and modeling of DC–DC converter
- (2) Under phase-shift control method for resonant mode of DC–DC converter, the turn-off current could be decreased, and the efficiency could be improved.

References

1. Zhang M, Liu J, Jin X (2011) Research on the FREEDM micro-grid and its relay protection. *Power Syst Prot Control* 39(7):95–99
2. Li L, Liu G (2011) Development of bi-directional DC–DC converter in multiple battery energy storage system. *Power Syst Prot Control* 39(3):90–94
3. Du C, Zhang C, Chen A et al (2011) Digital control and implementation of photovoltaic soft-switching DC–DC converter with high-frequency step-up transformer isolation. *Trans Chin Electrotech Soc* 26(8):57–63
4. Liu H, Mao C, Lu J et al (2010) Energy storage system of electronic power transformer and its optimal control. *Trans Chin Electrotech Soc* 25(3):54–60
5. Demetriades GD, Nee HP (2008) Small-signal analysis of the half-bridge soft-switching unidirectional converter employing extended state-space averaging. In: *Power electronics specialists conference, Rhodes*, pp 385–391
6. Demetriades GD, Nee HP (2008) Characterization of the dual-active bridge topology for high-power applications employing a duty-cycle modulation. In: *Power electronics specialists conference, Rhodes*, pp 2791–2798
7. Bai H, Nie Z, Chris CM (2010) Experimental comparison of traditional phase-shift, dual-phase-shift, and model-based control of isolated bidirectional DC–DC converters. *IEEE Trans Power Electron* 25(6):1444–1449
8. Oggier GG, Gar'cia GO, Oliva AR (2009) Switching control strategy to minimize dual active bridge converter losses. *IEEE Trans Power Electron* 24(7):1826–1838
9. Ortiz G, Biela J, Bortis D et al (2010) 1 megawatt, 20 kHz, isolated, bidirectional 12 kV to 1.2 kV DC–DC converter for renewable energy applications. In: *Power electronics conference, Singapore*, pp 3212–3219
10. Lenke R, Mura F, De Doncker RW (2009) Comparison of non-resonant and super-resonant dual-active ZVS-operated high-power DC–DC converters. In: *European conference on power electronics and applications*, 2009, pp 1–10
11. Li X, Ashoka KSB (2010) Analysis and design of high-frequency isolated dual-bridge series resonant DC–DC converter. *IEEE Trans Power Electron* 25(4):850–862
12. Wu L, Zhang Y, Li Z, Wang P, Li Y, Liu Z (2012) A control strategy of isolated bidirectional full bridge DC/DC converter. *Electric Mach Control* 16(12):21–27

Proceedings of the 2013 International Conference on
Electrical and Information Technologies for Rail
Transportation (EITRT2013)-Volume II

Jia, L.; Liu, Z.; Qin, Y.; Zhao, M.; Diao, L. (Eds.)

2014, XV, 615 p. 342 illus., Hardcover

ISBN: 978-3-642-53750-9